



## OPTIMAL DESIGN OF NON-PRISMATIC REINFORCED CONCRETE BOX GIRDER BRIDGE: MINIMIZATION OF THE COST AND CO<sub>2</sub> EMISSION

L. Mottaghi<sup>1\*</sup>, †, A. Kaveh<sup>2</sup> and R. A. Izadifard<sup>1</sup>

<sup>1</sup>*Civil Engineering Department, Imam Khomeini International University, Qazvin, Iran*

<sup>2</sup>*School of Civil Engineering, Iran University of Science and Technology, Tehran, Iran*

### ABSTRACT

This paper presents a computational framework for optimal design of non-prismatic reinforced concrete box girder bridges. The variables include the geometry of the cross section, tapered length, concrete strength and reinforcement of box girders and slabs. These are obtained by the enhanced colliding bodies optimization algorithm to optimizing the cost and again CO<sub>2</sub> emission. Loading and design is based on the AASHTO standard specification. The methodology is illustrated by a three-span continuous bridge. The trade-off between optimal cost and CO<sub>2</sub> emission in this type of bridge indicates that the difference of costs, as well as CO<sub>2</sub> emissions in the solution with both objectives is less than 1%. However, the optimal variables in the cost objective are different from the variables of CO<sub>2</sub> emission objective.

**Keywords:** optimal cost; optimal CO<sub>2</sub> emissions; RC box girder bridge; non-prismatic; ECBO algorithm.

Received: 24 August 2022; Accepted: 5 November 2022

### 1. INTRODUCTION

In traditional trial and error-based design, the analysis of structure is repeated until a reasonable design is attained. But the design obtained with this method is not sufficient to achieve both economy and safety simultaneously. Using optimization methods is intelligent way to explore the optimal solution of a large search space of problems. Many studies have been performed on the optimal design of bridge to minimize the economic costs. Perea *et al.* (2008) minimized the cost of reinforced concrete box frames bridge by using four heuristic

---

\*Corresponding author: Civil Engineering Department, Imam Khomeini International University, Qazvin, Iran

†E-mail address: lidamottaghi@yahoo.com (L. Mottaghi)

algorithms. Aydın and Ayvaz (2013) presented a method to optimize the cost of prestressed concrete I-girder bridges by using genetic algorithm. Srinivas and Ramanjaneyulu (2007) used genetic algorithms and artificial neural networks to optimize the cost of T-girder bridge deck. Kaveh *et al.* (2016) implemented three metaheuristics algorithm to optimize the cost of post-tensioned concrete box girder of single span bridges. The constraints were based on AASHTO standard specifications and construction limitations. Pedro *et al.* (2017) describes a two-stage optimization approach for designing steel-concrete composite I-girder bridges to minimize the material costs. Yavari *et al.* (2016) investigated the automatic design and structural optimization of concrete slab frame bridges with the aim of reducing the cost. They used the Genetic algorithm and pattern search method for optimization. Kaveh (2006) presented 25 different metaheuristic optimization algorithms. Kaveh and Adadi (2020) provided optimization of composite floors. Kaveh *et al.* (2019) compared the performance of three metaheuristic algorithms in design of the steel-concrete composite I-girder bridges. Yepes *et al.* (2019) optimized the economic cost of the post-tensioned concrete box-girder pedestrian deck, with the loading and design being based on Spanish code. Penadés Plà *et al.* (2020) presented a robust optimization method to design a continuous prestressed concrete box girder pedestrian bridge. Kaveh *et al.* (2022)(a) describes a methodology for optimal design of reinforced concrete 3D columns and bent caps of bridges. Kaveh *et al.* (2022)(b) compared the performance of three metaheuristic algorithms (WSA, ECBO, EVPS) in optimal design of bridge.

In previous studies, the objective function in the optimal design was minimizing the cost, though the environmental impact of the construction industry on greenhouse gases was also important. Researchers have used strategies to reduce these effects utilizing optimization techniques. Reinforced concrete structures are made of two type material, concrete and steel, that have different amount of carbon dioxide emission during the construction phase. Thus, RC structures have high potential to minimize CO<sub>2</sub> emissions. Many studies are performed on the RC frame with the objective of minimizing CO<sub>2</sub> emission (Eleftheriadis *et al.* 2018, Khajehzadeh *et al.* 2013, Khajehzadeh *et al.* 2014, Kaveh *et al.* 2020, Kaveh *et al.* 2021, Kaveh *et al.* 2022(c), Mottaghi *et al.* 2020, Oh *et al.* 2016, Park *et al.* 2018). Limited studies have also been conducted on the bridges to reduce the CO<sub>2</sub> emissions. Yepes *et al.* (2015) has proposed an optimal design method to minimize the cost and CO<sub>2</sub> emission for precast–prestressed bridges with a double U-shape cross-section. They used high strength concrete as well as self-compacting concrete in beams. They concluded that optimal solutions in terms of monetary costs are slightly different from the environmental solutions. García-Segura *et al.* (2015) optimally designed the post-tensioned concrete box-girder pedestrian bridges with the cost and CO<sub>2</sub> emission objectives. They showed that the environmental objectives also ensure economic solutions. García-Segura and Yepes (2016) have used a multi-objective harmony search algorithm to optimal design post-tensioned concrete road bridges in order to reduce CO<sub>2</sub> emissions and cost and overall safety factor.

A review of the literature shows that no study has been conducted on optimal design of reinforced concrete bridges with non-prismatic deck. In this paper, a process is described for optimal design the superstructure of multi-span non-prismatic reinforced concrete box girder bridges. The link of CSiBridge and MATLAB software are used for the optimization process. Where CSiBridge software is used for finite element analysis. The AASHTO (2002) standard specification and optimization algorithm are handled in MATLAB software.

The objective functions are considered to optimize the cost or CO<sub>2</sub> emissions. The aim of this study is two folds. To provide a methodology for optimal design of multi-span 3D non-prismatic reinforced concrete box girder bridges. And to investigate the tradeoff between optimal cost and optimal CO<sub>2</sub> emission in this type of bridges.

After this introduction, the formulation of optimal design is presented in Sect. 2. A brief explanation of the algorithm used in this paper is presented in Sect. 3. Numerical example and the results are studied in Sect. 4. Finally, conclusions are presented in Sect. 5.

## 2. FORMULATION OF OPTIMAL DESIGN

In this section, the optimization method for 3D reinforced concrete bridges with non-prismatic deck and several spans (Fig. 1) is studied.

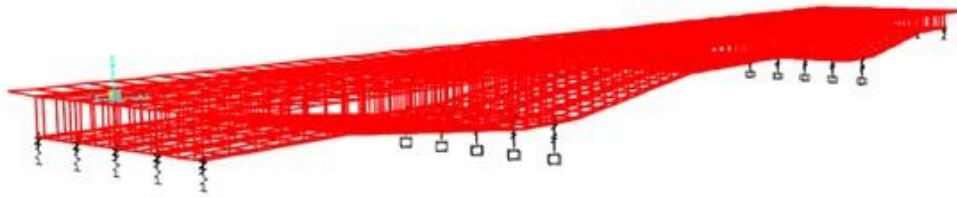


Figure 1. Non-prismatic RC bridge

### 2.1 Design variables

Design variables during the optimization process are concrete strength, geometry of the cross sections, tapered lengths, reinforcement of the box girders and slabs. The variables are tabulated in Table 1, and geometry of the cross-section of the bridge with some of the variables are shown in Fig. 2.

Table 1: Design variables and parameters

| No. | variables and parameters                                | Symbol   | step | Variable bounds          |
|-----|---|----------|------|--------------------------|
| 1   | Concrete strength (kg/cm <sup>2</sup> )                 | $f'_c$   | 50   | $350 \leq f'_c \leq 500$ |
| 2   | Girder depth (m)  | $h1, h3$ | 0.25 | $1 \leq h \leq 3$        |
| 3   | Girder depth in the mid supports (m)                    | $h2$     | 0.25 | $1.5 \leq h \leq 3.5$    |
| 4   | Top slab thickness (cm)                                 | $T_t$    | 1    | $18 \leq T_t \leq 35$    |
| 5   | Bottom slab thickness (cm)                              | $T_b$    | 1    | $17 \leq T_b \leq 30$    |
| 6   | End thickness of cantilever (cm)                        | $T_c$    | 1    | $18 \leq T_c \leq 30$    |
| 7   | Initial thickness of cantilever (cm)                    | $T_s$    | 2    | $20 \leq T_s \leq 50$    |
| 8   | Length of cantilever (m)                                | $L_c$    | 0.25 | $1 \leq L_c \leq 2.25$   |
| 9   | Web thickness in intermediate cell (cm)                 | $T_{W3}$ | 2    | $25 \leq T_{W1} \leq 50$ |
| 10  | Web thickness in outside cell (cm)                      | $T_{W1}$ | 2    | $30 \leq T_{W1} \leq 70$ |
| 11  | Diameter of bars perpendicular to traffic in slabs      | $d_1$    | 1    | $\#3 \leq d_1 \leq \#11$ |
| 12  | Number of bars perpendicular to traffic in slabs        | $n_1$    | 1    | $2 \leq n_1 \leq 15$     |
| 13  | Diameter of bars perpendicular to traffic in cantilever | $d_2$    | 1    | $\#3 \leq d_2 \leq \#11$ |

|    |  |       |          |                          |
|----|--|-------|----------|--------------------------|
| 14 | Number of bars perpendicular to traffic in cantilever        | $n_2$ | 1        | $2 \leq n_2 \leq 15$     |
| 15 | Number of longitudinal bars in moment capacity for girders   | $n_l$ | 1        | $2 \leq n_l \leq 15$     |
| 16 | Diameter of longitudinal bars in moment capacity for girders | $d_l$ | 2        | $\#3 \leq d_l \leq \#11$ |
| 17 | Diameter of shear bars (mm)                                  |       | constant | #4                       |
| 18 | Tapered length (TLR) (m)                                     | TLR   | 1        | $3 \leq TLR \leq 9$      |
| 19 | $t_1=t_2=t_3=t_4=t_5=t_6=t_7=t_8$ (mm)                       |       | constant | 150                      |
| 20 | Number of cells  |       | constant | 4                        |

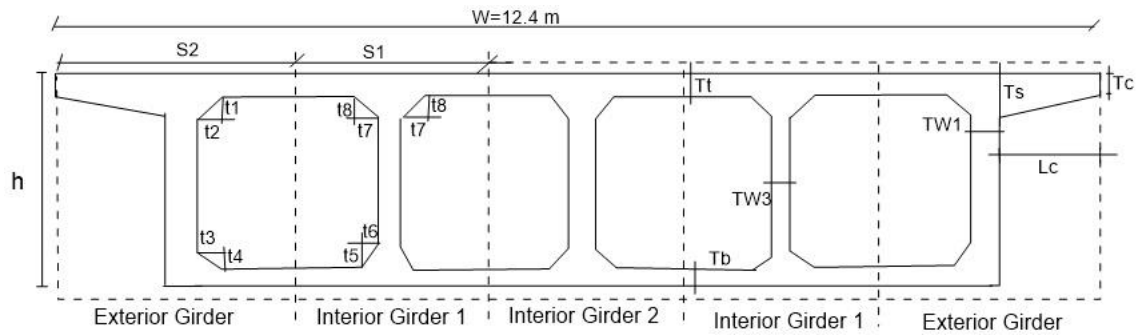


Figure 2. Geometry of the superstructure

2.2 Loading

Maximum compressive and tensile responses in girders are provided by permanent dead load and live loads. Dead loads include the weight of girders and slabs as well as the weight of the asphalt. The weight per unit volume of concrete is 2.5 ton / m<sup>3</sup> and the weight per unit volume of the asphalt is 2.2 ton / m<sup>3</sup>. The cover on the bars is assumed to be 5 cm and the thickness of the asphalt is 5 cm. According to the Articles 3.7 from the AASHTO 2002, H20-44 and HS20-44 live load are considered, that are shown in Fig. 3. These loads are placed in 3.6 m traffic lanes. The width of the deck is 12.4 meter and the number of traffic lanes is considered as 3.

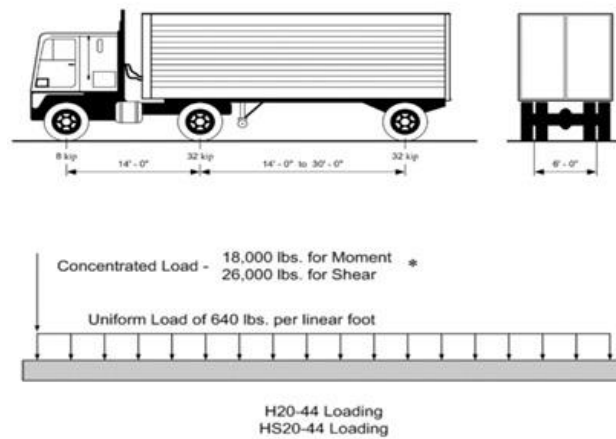


Fig. 3 Live loads

The combination of loads according of TABLE 3.22.1A AASHTO that is considered for design of the deck are as follows:

$$\text{Combination load} = 1.3DL + 2.17LL \quad (1)$$

where DL is dead load and LL is a live load. When traffic lanes are loaded simultaneously, the percentage of the live load should be considered in loading. In this example, this factor according Article 3.12 from the AASHTO 2002 is equal to 0.9. Live loads are multiplied by a coefficient called the dynamic impact factor. This factor is calculated according to the following equation:

$$MI = 1 + \frac{50}{3.28L + 125} \leq 1.3 \quad (2)$$

where L is the length of the span in meter.

### 2.3 Methodology of optimal design

The link of CSiBridge v22.1 and Matlab 2016a have been used for optimization. CSiBridge software is used for finite element analysis and MATLAB software has been used to optimize and verification the AASHTO 2002 standard specification. First, a bridge model is constructed according to the desired specifications in CSiBridge and its text file (\$br) is saved. The variables of problem are defined in the br file and stored in MATLAB. The information in this document is updated in each iteration. The CSiBridge imports the information of this file and perform its analysis. OAPI functions have been used to link softwares, analyze 3D model and extract results. The flowchart for this process is shown in Fig. 4. The shell element is used to model the deck. In the finite element mesh, the maximum segment length is taken as 1m to extract the results and the maximum submesh size is 1.2 m. In order to save the solution time, the program does not enter the analysis stage until the limitations of slab design of the deck and geometry constraints are satisfied.

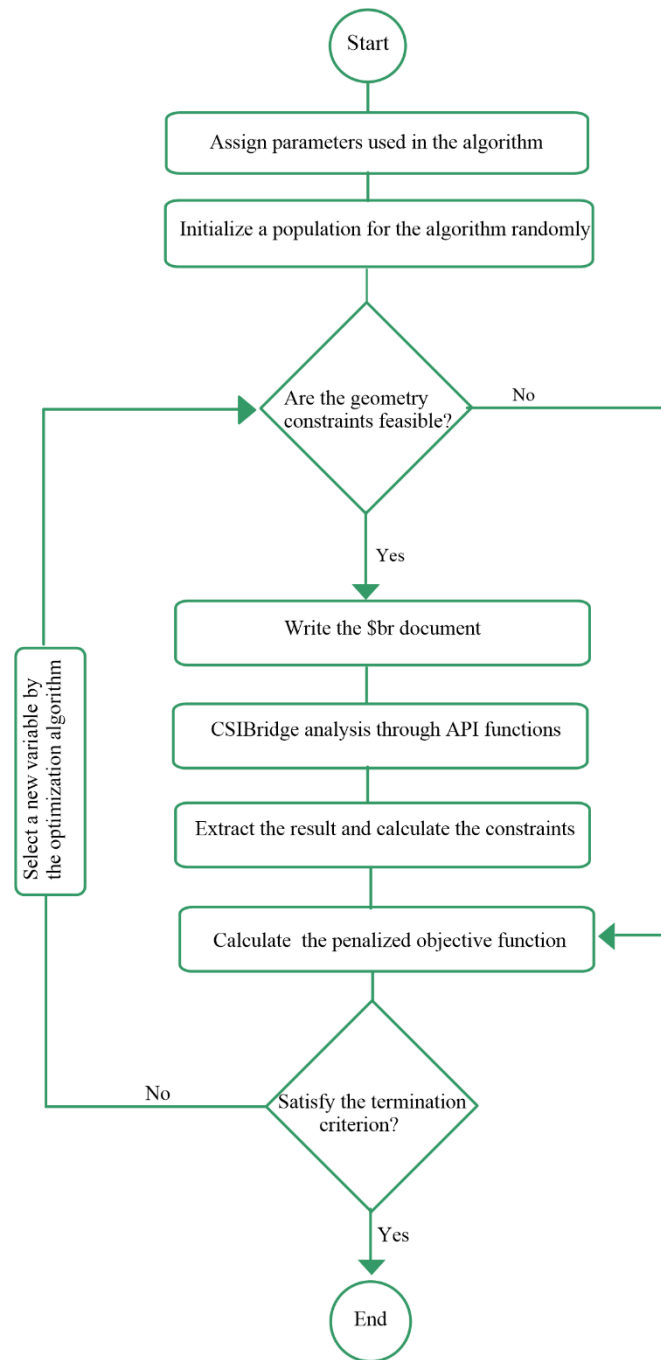


Figure 4. Flowchart of the proposed optimization framework

#### 2.4 Design constraints

The design of the bridge is based on specification of the AASHTO 2002. In this study, the units are considered as ton and meter.

In the longitudinal design of the deck (girders), flexural moment and shear force in

different sections along the bridge are obtained from CSiBridge software and compared with flexure and shear constraints. The constraints are expressed in the following.

#### 2.4.1 Flexure constraints

For any section of a flexural member, the sections are designed to resist the applied bending moments. The constraints are controlled for the positive bending moments and the negative bending moments of the box girder sections. The penalty function for the moment capacity of sections is calculated as:

$$g_1 = \frac{|M_u| - \phi M_n}{\phi M_n} \quad (3)$$

where  $M_u$  is the applied ultimate bending moment,  $\phi$  is the strength reduction factor which is equal 0.9. Article 8.16 from the AASHTO 2002 (strength design method) has been used to calculate the nominal flexural strength capacity ( $M_n$ ).

$M_n$  of a rectangular beam section is defined as follows:

$$M_n = A_s f_y \left( d - \frac{a}{2} \right) \quad (4)$$

$$a = \frac{A_s f_y}{0.85 f'_c b} \quad (5)$$

where  $A_s$  is the total area of tensile reinforcing bars,  $f_y$  is the yield strength of reinforcing bars,  $d$  is the distance from extreme compression fiber to the centroid of tension reinforcing bars, and  $a$  is the depth of the equivalent rectangular stress block.

The balanced reinforcement ratio  $\rho_b$  is calculated as

$$\rho_b = 0.85 \beta_1 \frac{f'_c}{f_y} \frac{60000}{60000 + f_y} \quad (6)$$

when the compression flange thickness is equal to or greater than the depth of the equivalent rectangular stress block,  $a$ , the design moment strength is calculated by Eq. (4).

When the compression flange thickness is less than  $a$ , the design moment strength is calculated as follow:

$$M_n = (A_s - A_{sf}) f_y \left( d - \frac{a}{2} \right) + A_{sf} f_y \left( d - \frac{h_f}{2} \right) \quad (7)$$

$$A_{sf} = \frac{0.85 f'_c (b - b_w) h_f}{f_y} \quad (8)$$

$$a = \frac{(A_s - A_{sf}) f_y}{0.85 f'_c b_w} \quad (9)$$

The balanced reinforcement ratio  $\rho_b$  in this stage is calculated as follows:

$$\rho_b = \left[ \left( 0.85 \beta_1 \frac{f_c}{f_y} \frac{60000}{60000 + f_y} \right) + \frac{A_{sf}}{b_w d} \right] \left( \frac{b_w}{b} \right) \quad (10)$$

The  $\beta_1$  stress block factor is taken as 0.85 for concrete strengths up to and including 28 MPa. For strengths above 28 MPa,  $\beta_1$  is calculated as:

$$\beta_1 = \max \left( 0.85 - \frac{f_c - 28}{7} 0.05, 0.65 \right) \quad (11)$$

The constraint of the maximum reinforcement section of beams is:

$$g_2 = \rho - 0.75 * \rho_b \quad (12)$$

The minimum distance between bars and minimum reinforcement section of beams are controlled according to the ACI (2008) code.

The penalty of the minimum distance between bars is:

$$s_{min} = \max(d_b, 25mm) \quad g_3 = \frac{s_{min} - s_l}{s_{min}} \quad (13)$$

where the  $d_b$  is the diameter of the bars and  $s_l$  is the distance between the longitudinal bars.

The constraint of the minimum reinforcement section of beams is:

$$\rho_{min} = \max \left( \frac{\sqrt{f'_c}}{0.4f_y}, \frac{140}{f_y} \right) \quad g_4 = \rho_{min} - \rho \quad (14)$$

#### 2.4.2 Shear constraints

The design of the sections under shear loads should be as follows:

$$V_u \leq \phi V_n \quad (15)$$

$$V_n = V_c + V_s \quad (16)$$

The constraints related to shear strength are as follows:

$$g_5 = \frac{|V_u| - \phi V_n}{\phi V_n} \quad (17)$$

where  $V_u$  is the applied shear force at the section,  $V_n$  is the nominal shear strength and  $\phi$  is the shear strength reduction factor which is equal to 0.85.

The  $V_c$  is the nominal shear strength provided by the concrete, that is calculated as:

$$V_c = 1.7 * \sqrt{f_c} b_w d \text{ (ton)} \quad (18)$$

The  $V_s$  is the nominal shear strength provided by the shear reinforcement, which is

calculated as:

$$V_s = \frac{A_V f_y \cdot d}{S} \quad (19)$$

where  $A_V$  is the area of shear reinforcement according to Table 1.

According to Article 8.19 from the AASHTO 2002, the minimum shear rebars are:

$$A_{Vmin} = \frac{35 \cdot b_w S}{f_y} (m^2) \quad (20)$$

where  $b_w$  is web width and  $S$  is spacing of shear reinforcement.

In order to consider the constraint of minimum shear reinforcement, the maximum  $A_V$  and  $A_{Vmin}$  values are considered for the design.

The distance between the shear rebars ( $S$ ) should not be greater than the following values:

$$S_{max} \leq \min\left(\frac{d}{2}, 0.6m\right) \quad (21)$$

$$g_6 = S - S_{max} \quad (22)$$

Sections located in the area less than  $d$  from the face of support, are designed for the same shear force in  $d$  area.

#### 2.4.3 Constraints for design of slab

According to Article 3.24 from the AASHTO, to calculate the main reinforcement perpendicular to traffic, the bending moment per meter of slab must be calculated as follows:

$$M_d = \frac{q \cdot S_1^2}{10} \left(\text{ton} \cdot \frac{m}{m}\right) \quad (23)$$

$$M_L = 0.8 \frac{1.64S_1 + 1}{16} P \left(\text{ton} \cdot \frac{m}{m}\right) \quad (24)$$

where  $S_1$  presents the length of the span (Fig. 2).  $M_d$  is the moment of the dead loads.  $M_L$  is the moment of the live loads.  $P$  is load on the rear wheel of the truck, which is considered equal to 7.25 tons. The flexural capacity is calculated according to Eq. (4). For the top slab, the minimum and maximum permissible percentage of bars is also controlled.

For lateral distribution of the concentrated live loads, the reinforcements should be placed at the bottom of the slab and perpendicular to the main reinforcement. The amount of distribution reinforcement ( $A_{sl}$ ) should be calculated as the percentage of the main reinforcement ( $A_{sv}$ ) according Article 3.24.10 from the AASHTO.

$$\frac{A_{sl}}{A_{sv}} = \frac{120}{\sqrt{S_1}} \quad (25)$$

$$A_{sl} = A_{sv} * \min\left(\frac{1.2}{\sqrt{S_1}}, 0.67\right) \quad (26)$$

According to the Article 8.17.2.3 from the AASHTO in the bottom flange of girder with box cross section, minimum longitudinal reinforcement of 0.4% of the flange area shall be placed parallel to the girder span. Minimum distributed reinforcement of 0.5% of the cross-sectional area of the slab, should be placed in the bottom slab transverse to the girder span.

According to Article 8.17.2.1.3 from the AASHTO, if the depth of the side face of a member exceeds of 1m, the area of longitudinal skin reinforcement per unit of height on each side face is  $\max(150, (d-750)) \text{ mm}^2$ .

#### 2.4.4 Geometry constraints

The bottom slab thickness limitation of a box girder according to Article 8.11.2 from the AASHTO is:

$$Tb_{min} = \max\left(\frac{S_1}{16}, 0.14\text{m}\right) \quad (27)$$

$$g_7 = \frac{Tb_{min} - Tb}{Tb} \quad (28)$$

The thickness of the bottom slab ( $Tb$ ) should not be more than that of the top slab ( $Tt$ ).

$$g_8 = \frac{Tb - Tt}{Tt} \quad (29)$$

The depth of the girders in areas near the supports should be greater than other areas:

$$g_9 = \frac{h_1 - h_2}{h_2} \quad (30)$$

$$g_{10} = \frac{h_3 - h_2}{h_2} \quad (31)$$

where the  $h_1$  and  $h_3$  is the depth of girders in first and mid spans, respectively.  $h_2$  is the depth of girders in mid supports.

And

$$g_{11} = \frac{T_c - T_s}{T_s} \quad (32)$$

#### 2.4.5 Slab deflection constraint

According to Article 8.9.3 from the AASHTO 2002 in the continuous spans the deflection due to service live load plus impact should not exceed 1/800 of the span ( $L$ ). The constraint for this item is as follow:

$$g_{12} = \frac{\Delta_g - \frac{1}{800}L}{\frac{1}{800}L} \quad (33)$$

Deflection of cantilever arms is limited as follows:

$$g_{13} = \frac{\Delta_c - \frac{1}{300}Lc}{\frac{1}{300}Lc} \quad (34)$$

### 2.5 Object functions

The objective of optimization is economic cost and the CO<sub>2</sub> emissions. The general form of both objective functions is presented by Eq. (35), where the unit rate of components varies for the cost and CO<sub>2</sub> emission objectives.  $C_c$ ,  $C_s$  and  $C_f$  are the unit rate of concrete, bars and formwork, respectively. Their values for the objective functions are given in Table 2.  $V_c$  is the volume of concrete, that is extract from the CSiBridge software;  $\gamma_s$  is unit weight of bars that is 7850 kg/m<sup>3</sup>;  $A_s$  and  $L_s$  are the area and length of bars, respectively;  $A_f$  is area of formwork. In this study, the weight of shear reinforcement is not considered in the objective functions.

$$C = (V_c \cdot C_c + C_s \cdot \gamma_s \cdot A_s \cdot L_s + C_f \cdot A_f) \quad (35)$$

Table 2 Unit prices and CO<sub>2</sub> emissions (García-Segura and Yepes 2016)

| Description                         | Cost (€) | Emission (kg CO <sub>2</sub> ) |
|-------------------------------------|----------|--------------------------------|
| kg of Steel B-500                   | 1.16     | 3.03                           |
| m <sup>3</sup> of Concrete (35 MPa) | 104.57   | 321.92                         |
| m <sup>3</sup> of Concrete (40 MPa) | 109.33   | 338.9                          |
| m <sup>3</sup> of Concrete (45 MPa) | 114.10   | 355.88                         |
| m <sup>3</sup> of Concrete (50 MPa) | 118.87   | 372.86                         |
| m <sup>2</sup> of Formwork          | 33.81    | 2.08                           |

### 3. OPTIMIZATION ALGORITHM

In this study, the enhanced colliding bodies optimization (ECBO) (Kaveh and Ghazaan 2014) algorithm is used to optimize the problem. ECBO algorithm have been used in several research in order to obtain optimal solutions (Fathali *et al.* 2020, Fathali and Hoseini Vaez 2020, Kaveh *et al.* 2017, Kaveh 2021). In the previous studies (Kaveh, Izadifard *et al.* 2020, Kaveh, Mottaghi, *et al.* 2020, Kaveh and Vazirinia 2018), the comparison of algorithms has shown that ECBO algorithm has better performance, so in this study we used this algorithm to obtain optimal solutions. This algorithm is modified version of the colliding bodies optimization (CBO) algorithm (Kaveh and Mahdavi 2014). These algorithms are inspired by the collision theory between two bodies. The specified mass of each colliding body is defined as:

$$m_k = \frac{1}{\frac{fit(k)}{\sum_{i=1}^n \frac{1}{fit(i)}}}, \quad k = 1, 2, \dots, n \quad (36)$$

where  $fit(i)$  represents the objective function value of the  $i$ th colliding body and  $n$  is the number of populations. The objects are sorted according to their weights in a decreasing order and divided into two equal groups, (i) stationary group and (ii) moving group. The moving object moves to the stationary object and a collision occurs, (Fig. 5). The new positions of the objects are updated by using the generated velocities after the collision and their old position.

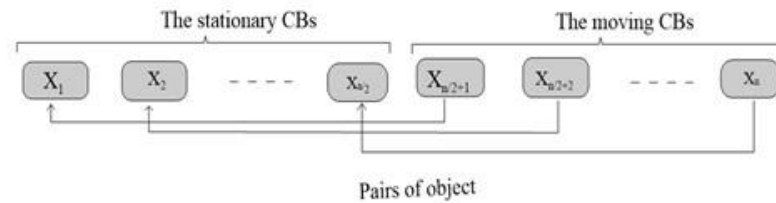


Figure 5. The pairs of objects for collision, (Kaveh and Ghazaan 2014)

Two techniques are used in ECBO algorithm to enhance the performance of CBO algorithm. One of them is collision memory ( $CM$ ), it stores some of the best solutions of every iteration found in the previous population and substitutes them with the worst CBs in the current population. In the second technique, one dimension of the  $i$ th CB will be randomly regenerated in each iteration. The probability of choosing this component is expressed by the  $Pro$  parameter. This parameter is within  $(0, 1)$  (Kaveh and Ghazaan 2014).

#### 4. DESIGN EXAMPLE

In order to investigate the objectives, which include minimizing the cost and CO<sub>2</sub> emissions, as well as to evaluate the proposed process for optimal design, a box girder reinforced concrete bridge is considered. The deck of the bridge has variable height, which is continuous on three spans with lengths of 18, 36 and 18 meters symmetrically. Fig. 6 illustrates the division of bridge for design. The beams are divided into 16 parts (section cuts) and 10 sections to satisfy the design and construction constraints.

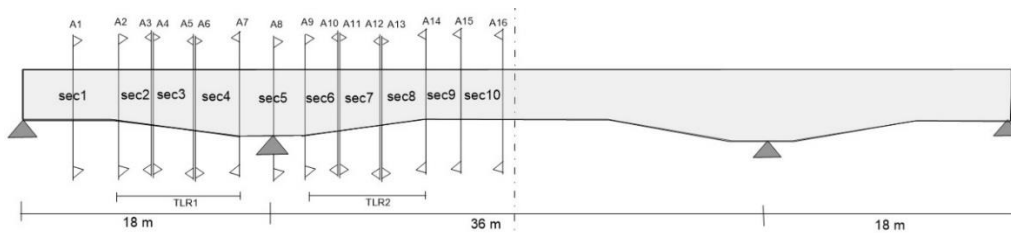


Figure 6. Bridge division for design

In this example, the variables expressed in Table 1 are the same in all the different sections, except for the items listed in Table 3. In this table, *htlr* is obtained for non-prismatic sections by interpolation.

Table 3 Segments and related variables

| Section cut | Depth of girders (h) | Number of longitudinal bars (top) | Diameter of longitudinal of bars (top) | Number of longitudinal bars (bottom) | Diameter of longitudinal bars (bottom) | Space of shear bar (S) |
|-------------|----------------------|-----------------------------------|--|--------------------------------------|--|------------------------|
| A1          | h1                   | nLt1                              | dLt1                                   | nLb1                                 | dLb1                                   | S1                     |
| A2          | h1                   | nLt2                              | dLt2                                   | nLb2                                 | dLb2                                   | S2                     |
| A3          | htlr1                | nLt2                              | dLt2                                   | nLb2                                 | dLb2                                   | S2                     |
| A4          | htlr1                | nLt3                              | dLt3                                   | nLb3                                 | dLb3                                   | S3                     |
| A5          | htlr2                | nLt3                              | dLt3                                   | nLb3                                 | dLb3                                   | S3                     |
| A6          | htlr2                | nLt4                              | dLt4                                   | nLb4                                 | dLb4                                   | S4                     |
| A7          | h2                   | nLt4                              | dLt4                                   | nLb4                                 | dLb4                                   | S4                     |
| A8          | h2                   | nLt5                              | dLt5                                   | nLb5                                 | dLb5                                   | S5                     |
| A9          | h2                   | nLt6                              | dLt6                                   | nLb6                                 | dLb6                                   | S6                     |
| A10         | htlr3                | nLt6                              | dLt6                                   | nLb6                                 | dLb6                                   | S6                     |
| A11         | htlr3                | nLt7                              | dLt7                                   | nLb7                                 | dLb7                                   | S7                     |
| A12         | htlr4                | nLt7                              | dLt7                                   | nLb7                                 | dLb7                                   | S7                     |
| A13         | htlr4                | nLt8                              | dLt8                                   | nLb8                                 | dLb8                                   | S8                     |
| A14         | h3                   | nLt8                              | dLt8                                   | nLb8                                 | dLb8                                   | S8                     |
| A15         | h3                   | nLt9                              | dLt9                                   | nLb9                                 | dLb9                                   | S9                     |
| A16         | h3                   | nLt10                             | dLt10                                  | nLb10                                | dLb10                                  | S10                    |

Tables 4 and 5 show the optimal results for the reinforcement and section design of bridge. The objective function is minimizing the economic cost. The volume of concrete in this solution is 513.0511m<sup>3</sup> and the total weight of the bars in slabs and girders are 64643.8 kg. Fig. 7 shows the convergence curve of the algorithm corresponding to the lowest cost. The best solution reported by the ECBO algorithm is 168473.4 Euro, with 363483 kg of CO<sub>2</sub> emission.

Table 4 Optimum longitudinal bars, depth of girders and also space of shear bars for cost objective

| Section | Girders            |                       |      |                    |                       |      |                    |                       |      | Depth(m) |          |
|---------|--------------------|-----------------------|------|--------------------|-----------------------|------|--------------------|-----------------------|------|----------|----------|
|         | Exterior Girder    |                       |      | Interior Girder 1  |                       |      | Interior Girder 2  |                       |      | h node i | h node j |
|         | A <sub>s</sub> top | A <sub>s</sub> bottom | S(m) | A <sub>s</sub> top | A <sub>s</sub> bottom | S(m) | A <sub>s</sub> top | A <sub>s</sub> bottom | S(m) |          |          |
| Sec 1   | 9#7                | 7#7                   | 0.2  | 11#5               | 8#7                   | 0.4  | 13#5               | 5#9                   | 0.4  | 1        | 1        |
| Sec 2   | 5#9                | 5#9                   | 0.3  | 11#7               | 5#9                   | 0.4  | 11#7               | 4#9                   | 0.4  | 1        | 1.55     |
| Sec 3   | 7#11               | 7#9                   | 0.3  | 5#11               | 9#7                   | 0.4  | 5#11               | 9#7                   | 0.4  | 1.555    | 1.97     |
| Sec 4   | 11#9               | 7#9                   | 0.3  | 6#11               | 10#9                  | 0.4  | 12#9               | 12#7                  | 0.4  | 1.972    | 2.25     |
| Sec 5   | 8#11               | 8#9                   | 0.2  | 10#11              | 10#7                  | 0.3  | 8#11               | 5#11                  | 0.3  | 2.25     | 2.25     |
| Sec 6   | 14#7               | 9#9                   | 0.2  | 14#7               | 7#9                   | 0.3  | 9#9                | 9#9                   | 0.3  | 2.25     | 2.166    |
| Sec 7   | 7#9                | 13#7                  | 0.2  | 7#9                | 6#9                   | 0.3  | 5#11               | 11#9                  | 0.3  | 2.1666   | 2.083    |
| Sec 8   | 8#9                | 6#9                   | 0.2  | 11#7               | 9#7                   | 0.3  | 14#7               | 12#7                  | 0.4  | 2.083    | 2        |
| Sec 9   | 7#9                | 11#9                  | 0.3  | 11#7               | 8#11                  | 0.4  | 4#11               | 9#11                  | 0.4  | 2        | 2        |
| Sec 10  | 10#7               | 14#9                  | 0.6  | 4#11               | 14#9                  | 0.6  | 6#9                | 8#11                  | 0.6  | 2        | 2        |

Table 5 Optimum result for cost objective

|                  |   |     |
|------------------|---|-----|
|                  | $f'_c$ (kg/cm <sup>2</sup> )                                  | 350 |
|                  | $T_t$ (cm)  | 21  |
|                  | $T_b$ (cm)  | 17  |
|                  | $T_c$ (cm)  | 21  |
|                  | $T_s$ (cm)  | 28  |
|                  | $L_c$ (m)   | 2   |
| Optimum variable | $T_{W3}$ (cm)   | 29  |
|                  | $T_{W1}$ (cm)   | 30  |
|                  | Top slab reinforcement/m; ( $n_1, d_1$ )                      | 5#5 |
|                  | Cantilever slab reinforcement<br>/m; ( $n_2, d_2$ )           | 5#5 |
|                  | TLR1 (m)  | 9   |
|                  | TLR2 (m)  | 6   |
| Average          | € 172448.5  |     |
| Best solution    | Cost 168473.4 € (with 363483 kg of CO <sub>2</sub> emissions) |     |

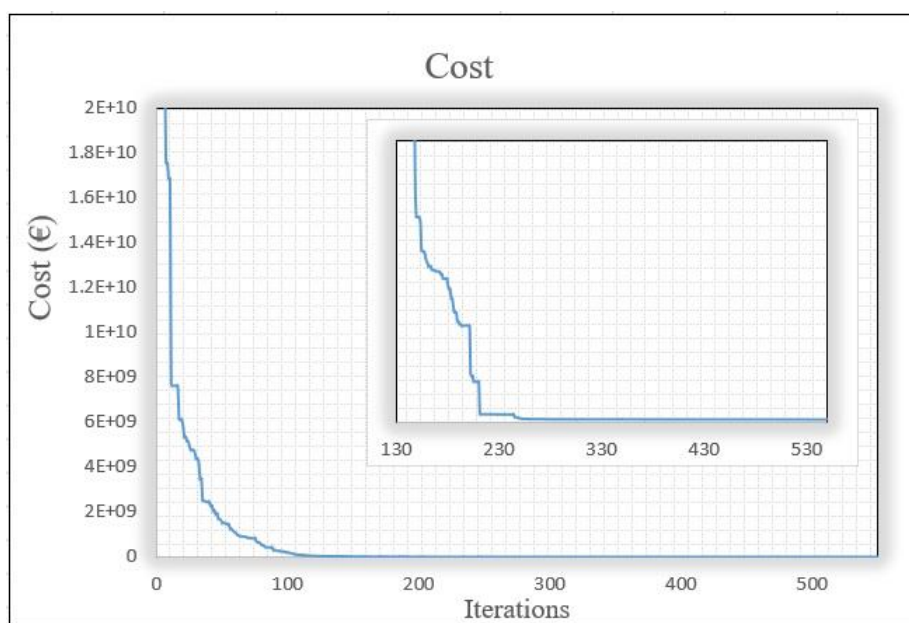


Figure 7. Convergence curve for lowest cost

The results of best design in minimizing CO<sub>2</sub> emissions are shown in Tables 6 and 7 for reinforcement and section design of bridge. The volume of concrete in this solution is 490.1887 m<sup>3</sup> and the total weight of bars in slabs and girders are 66685.8 kg. Fig. 8 shows the convergence curve for lowest CO<sub>2</sub> emission. The best reported solution is 362353.5 kg of CO<sub>2</sub> emissions with the cost of 169153.5 euro.

Table 6: Optimum longitudinal bars, depth of girders and also space of shear bars for CO<sub>2</sub> emissions objective

| Section | Girders            |                       |      |                    |                       |      |                    |                       |      | Depth(m) |          |
|---------|--------------------|-----------------------|------|--------------------|-----------------------|------|--------------------|-----------------------|------|----------|----------|
|         | Exterior Girder    |                       |      | Interior Girder 1  |                       |      | Interior Girder 2  |                       |      | h node i | h node j |
|         | A <sub>s</sub> top | A <sub>s</sub> bottom | S(m) | A <sub>s</sub> top | A <sub>s</sub> bottom | S(m) | A <sub>s</sub> top | A <sub>s</sub> bottom | S(m) |          |          |
| Sec 1   | 9#7                | 6#7                   | 0.4  | 14#5               | 5#9                   | 0.5  | 8#7                | 4#9                   | 0.5  | 1.25     | 1.25     |
| Sec 2   | 9#7                | 15#5                  | 0.4  | 9#7                | 9#7                   | 0.5  | 10#7               | 13#5                  | 0.5  | 1.25     | 1.718    |
| Sec 3   | 11#7               | 7#9                   | 0.4  | 8#9                | 10#7                  | 0.4  | 11#7               | 7#9                   | 0.5  | 1.718    | 2.187    |
| Sec 4   | 13#7               | 13#7                  | 0.4  | 8#9                | 8#9                   | 0.4  | 9#9                | 4#11                  | 0.5  | 2.187    | 2.5      |
| Sec 5   | 12#9               | 8#9                   | 0.3  | 11#9               | 4#11                  | 0.3  | 11#9               | 10#7                  | 0.3  | 2.5      | 2.5      |
| Sec 6   | 12#7               | 8#9                   | 0.3  | 12#7               | 7#9                   | 0.3  | 7#9                | 6#9                   | 0.3  | 2.5      | 2.333    |
| Sec 7   | 7#9                | 12#7                  | 0.3  | 11#7               | 6#9                   | 0.3  | 10#7               | 9#7                   | 0.3  | 2.333    | 2.1666   |
| Sec 8   | 10#7               | 6#9                   | 0.3  | 10#7               | 11#7                  | 0.4  | 13#7               | 11#7                  | 0.4  | 2.1666   | 2        |
| Sec 9   | 10#7               | 10#9                  | 0.3  | 5#9                | 6#11                  | 0.4  | 5#9                | 10#9                  | 0.5  | 2        | 2        |
| Sec 10  | 5#11               | 10#9                  | 0.6  | 4#11               | 13#9                  | 0.6  | 5#9                | 14#9                  | 0.6  | 2        | 2        |

Table 7: Optimum result for CO<sub>2</sub> objective

|                   |   |      |
|-------------------|---|------|
| Optimum variables | $f'_c$ (kg/cm <sup>2</sup> )                                    | 350  |
|                   | $T_t$ (cm)  | 18   |
|                   | $T_b$ (cm)  | 17   |
|                   | $T_c$ (cm)  | 21   |
|                   | $T_s$ (cm)  | 22   |
|                   | $L_c$ (m)   | 2    |
|                   | $T_{W3}$ (cm)   | 25   |
|                   | $T_{W1}$ (cm)   | 30   |
|                   | Top slab reinforcement/m; ( $n_1, d_1$ )                        | 10#4 |
|                   | Cantilever slab reinforcement/m; ( $n_2, d_2$ )                 | 10#4 |
| TLR1 (m)          | 8   |      |
| TLR2 (m)          | 6   |      |
| Average           | kg 370700.5   |      |
| Best solution     | CO <sub>2</sub> emissions 362353.5 kg (with 169153.5 € of cost) |      |

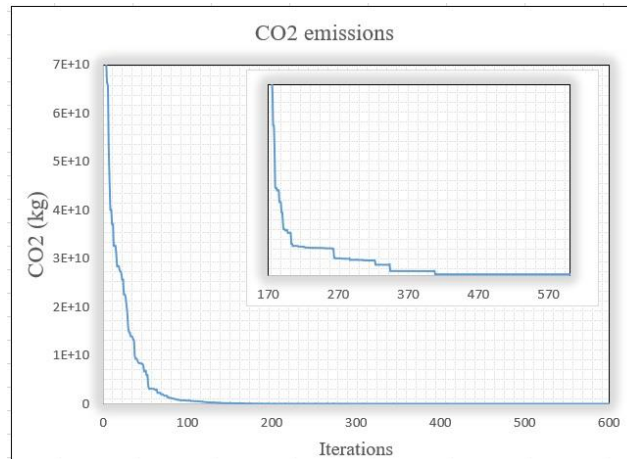


Figure 8. Convergence curve for lowest CO<sub>2</sub> emission

A comparison between the best solutions where the objective function is to minimize CO<sub>2</sub> emissions and one with the objective function being minimizing the cost shows that the difference of the cost (also CO<sub>2</sub>) in both objectives is less than 1%. Where in the cost objective function, the best cost is 168473.4 Euro with 363483 kg of CO<sub>2</sub> emission and in the solution with CO<sub>2</sub> emission objective function, the best CO<sub>2</sub> is 362353.5 kg with the cost of 169153.5 Euro. However, the optimal variables obtained in both objectives are different. The volume of concrete in the minimizing of cost is 513.051 m<sup>3</sup> and the total weight of bars is 64643.8 kg. In minimizing of CO<sub>2</sub> emission, the volume of concrete is 490.1887 m<sup>3</sup> and the weight of bars is 66685.8 kg. It can be useful for the decision maker in the select of variables according to the availability of materials. It is concluded that optimal solutions in cost objective are environmentally friendly design.

## 5. CONCLUDING REMARKS

Reinforced concrete structures have a great contribution in carbon dioxide emission. Recently, studies have been conducted on optimal design of structures with the aim of reducing CO<sub>2</sub> emission. Unfortunately, the number of these studies especially in the field of bridges design is limited. In this study, a method is proposed for optimal design of multi-span non-prismatic reinforced concrete box girder bridge with the aim of reducing costs and CO<sub>2</sub> emission. The link of CSiBridge and MATLAB software are used for the optimization process. CSiBridge software being employed for finite element analysis. The AASHTO 2002 standard specification and optimization algorithm are handled in MATLAB software. In this process, the design can be performed according to any desired specification standard. The variables considered in this work include concrete strength, tapered length, geometry, reinforcement of box girders and slabs. Constraints are the geometric, bending, shear and deflection limits. The process is implemented to optimal design of the deck of a 3D three-span bridge. The trade-off between optimal cost and CO<sub>2</sub> emission in this type of bridge indicates that, the optimal solutions obtained from the cost objective are also environmentally friendly design, and conversely the solutions of minimizing CO<sub>2</sub> emission have optimal cost.

## REFERENCES

1. AASHTO (2002). Standard Specifications for Highway Bridges, American Association of State Highway and Transportation Officials; Washington, DC.
2. ACI 318 (2008). Building code requirements for structural concrete and commentary, American Concrete Institute; Farmington Hills, MI, USA
3. Aydın Z, Ayvaz Y (2013). Overall cost optimization of prestressed concrete bridge using genetic algorithm, *KSCE J Civil Eng*; **17**(4): 769-76. doi.org/10.1007/s12205-013-0355-4.
4. Eleftheriadis S, Duffour P, Greening P, James J, Stephenson B, Mumovic D. Investigating relationships between cost and CO<sub>2</sub> emissions in reinforced concrete structures using a BIM-based design optimisation approach, *Ener Build* 2018; **166**: 330–

46. doi.org/10.1016/j.enbuild.2018.01.059.
5. Fathali MA, Dehghani E, Hoseini Vaez SR. An approach for adjusting the tensile force coefficient in equivalent static cable-loss analysis of the cable-stayed bridges, *Struct* 2020; **25**: 720–9. doi.org/10.1016/j.istruc.2020.03.054.
  6. Fathali MA, Hoseini Vaez SR. Optimum performance-based design of eccentrically braced frames, *Eng Struct* 2020; **202**. doi.org/10.1016/j.engstruct.2019.109857.
  7. García-Segura T, Yepes V. Multiobjective optimization of post-tensioned concrete box-girder road bridges considering cost, CO2 emissions, and safety, *Eng Struct* 2016; **125**: 325–36. doi.org/10.1016/j.engstruct.2016.07.012.
  8. García-Segura T, Yepes V, Alcalá J, Pérez-López E. Hybrid harmony search for sustainable design of post-tensioned concrete box-girder pedestrian bridges, *Eng Struct* 2015; **92**: 112–22. doi.org/10.1016/j.engstruct.2015.03.015.
  9. Kaveh A. *Advances in Metaheuristic Algorithms for Optimal Design of Structures*, 3rd edition, Springer, Switzerland, 2021.
  10. Kaveh A, Abadi ASM. Cost optimization of composite floor system using an improved harmony search algorithm, *J Construct Steel Res* 2010; **66**: 664–69.
  11. Kaveh A, Maniat M, Arab Naeni M. Cost optimum design of post-tensioned concrete bridges using a modified colliding bodies optimization algorithm, *Adv Eng Softw* 2016; **98**: 12–22. doi.org/10.1016/j.advengsoft.2016.03.003.
  12. Kaveh A, Mottaghi L, Izadifard RA. Optimization of columns and bent caps of RC bridges for cost and CO2 emission, *J Period Polytech Civil Eng* 2022a; doi.org/10.3311/PPci.19413.
  13. Kaveh A, Mottaghi L, Izadifard RA. Optimal design of a non-prismatic reinforced concrete box girder bridge with three meta-heuristic algorithms, *Iran J Sci Technol* 2022b; doi:10.24200/SCI.2022.59322.6178.
  14. Kaveh A, Mottaghi L, Izadifard RA. Sustainable design of reinforced concrete frames with non-prismatic beams, *Eng Comput* 2020; doi.org/10.1007/s00366-020-01045-4.
  15. Kaveh A, Mahdavi VR. Colliding bodies optimization : A novel meta-heuristic method, *Comput Struct* 2014; **139**: 18–27. doi.org/10.1016/j.compstruc.2014.04.005.
  16. Kaveh A, Mahdavi VR, Kamalinejad M. Optimal design of the monopole structures using the CBO and ECBO algorithms, *Period Polytech Civil Eng* 2017; **61**(1): 110–16. doi.org/10.3311/PPci.8546.
  17. Kaveh A, Motesadi Zarandi MM. Optimal design of steel-concrete composite I-girder bridges using three meta-heuristic algorithms, *Period Polytech Civil Eng* 2019; **63**(2): 317–37. doi.org/10.3311/PPci.12769.
  18. Kaveh A, Ilchi Ghazaan M. Enhanced colliding bodies optimization for design problems with continuous and discrete variables, *Adv Eng Softw* 2014; **77**: 66–75. doi.org/10.1016/j.advengsoft.2014.08.003
  19. Kaveh A, Izadifard RA, Mottaghi L. Optimal design of planar RC frames considering CO2 emissions using ECBO , EVPS and PSO metaheuristic algorithms, *J Build Eng* 2020; **28**. doi.org/10.1016/j.jobee.2019.101014.
  20. Kaveh A, Mottaghi L, Izadifard RA. An integrated method for sustainable performance-based optimal seismic design of RC frames with non-prismatic beams, *J Sci Iran* 2021; doi:10.24200/SCI.2021.58452.5728.
  21. Khajehzadeh M, Taha MR, Eslami M. Multi-objective optimization of foundation using

- global-local gravitational search algorithm, *Struct Eng Mech* 2014; **50**(3): 257–73. doi.org/10.12989/sem.2014.50.3.257.
22. Mottaghi L, Izadifard RA, Kaveh A. Factors in the relationship between optimal CO2 emission and optimal cost of the RC frames, *Period Polytech Civil Eng* 2021; **65**(1): 1–14. doi.org/10.3311/PPci.16790.
  23. Oh BK, Park JS, Choi SW, Park HS. Design model for analysis of relationships among CO2 emissions, cost, and structural parameters in green building construction with composite columns, *Ener Build* 2016; **118**: 301–15. doi.org/10.1016/j.enbuild.2016.03.015.
  24. Park HS, Hwang JW, Oh BK. Integrated analysis model for assessing CO2 emissions, seismic performance, and costs of buildings through performance-based optimal seismic design with sustainability, *Ener Build* 2018; **158**: 761–75. doi.org/10.1016/j.enbuild.2017.10.070
  25. Pedro RL, Demarche JL, Miguel FF, Lopez RH. An efficient approach for the optimization of simply supported steel-concrete composite I-girder bridges, *Adv Eng Softw* 2017; **112**: 31–45. doi.org/10.1016/j.advengsoft.2017.06.009.
  26. Perea C, Alcala J, Yepes V, Gonzalez-Vidosa F, Hospitaler A. Design of reinforced concrete bridge frames by heuristic optimization, *Adv Eng Softw* 2008; **39**(8): 676–88. doi.org/10.1016/j.advengsoft.2007.07.007.
  27. Penadés-Plà V, García-segura T, Yepes V. Robust design optimization for low-cost concrete box-girder bridge, *Mathemat* 2020; **8**(3): 1–14. doi: 10.3390/math8030398.
  28. Srinivas V, Ramanjaneyulu K. An integrated approach for optimum design of bridge decks using genetic algorithms and artificial neural networks, *Adv Eng Softw* 2007; **38**(7): 475–87. doi.org/10.1016/j.advengsoft.2006.09.016.
  29. Yavari MS, Pacoste C, Karoumi R. Structural Optimization of concrete slab frame bridges considering investment cost, *J Civil Eng Archit* 2016; **10**(9): 982–94. doi: 10.17265/1934-7359/2016.09.002.
  30. Yepes V, Martí JV, García-Segura T. Cost and CO2 emission optimization of precast-prestressed concrete U-beam road bridges by a hybrid glowworm swarm algorithm, *Autom Constr* 2015; **49**: 123–34. doi.org/10.1016/j.autcon.2014.10.013.
  31. Yepes V, Pérez-lópez E, García-segura T, Alcalá J. Optimization of high-performance concrete post-tensioned box-girder pedestrian bridge, *Int J Comp Meth Exp Meas* 2019; **7**(2): 118–29. doi: 10.2495/CMEM-V7-N2-118-129.